Metal nanostructures

3D Metallic Nanostructure Fabrication by Surfactant-Assisted Multiphoton-Induced Reduction**

Yao-Yu Cao, Nobuyuki Takeyasu, Takuo Tanaka, Xuan-Ming Duan,* and Satoshi Kawata*

A laser direct-writing technique employing multiphoton absorption processes has become a powerful and widely used tool in the fabrication of micro-/nanometer-scale structures in the past decade because of its 3D fabrication ability. Using this technique, a number of 2D and 3D microstructures have been successfully created with polymers,[1,2] glasses,[3] and metals.[4] In particular, since nanoscale metals exhibit unprecedented and unique properties such as electromagnetic field enhancement, catalysis, photoemission, and electronic conductivity[5–8] never found in their bulk states, metal structures with nanoscale geometries have received much attention from various fields such as plasmonics,[9–11] electronics,[12] bioscience,[13] and chemistry.[14–16] Although progress has been made in the fabrication of metal structures using lasers,[17–19] it is still challenging to obtain the nanometer-scale resolution required for fabricating continuous and fine metallic structures.

Up to today, three types of media have been mainly reported for fabricating metallic structures patterned by multiphoton-induced photoreduction. For example, Wu et al. demonstrated the fabrication of 3D metallic structures with micrometer resolution in a sol–gel matrix.[20] Stellacci et al. showed 3D continuous metallic structures fabricated by direct laser writing in polymer composites containing metal nanoparticles and a silver salt ($AgBF_4$).[21] In our previous report,[22] we demonstrated that silver wires could be directly fabricated in an aqueous solution of silver ions. In that study, Coumarin 440 was adopted to avoid a heating effect by partially converting laser energy to chemical energy or fluorescence, since the strong thermal reduction of the silver ions degraded the metal structure. Although many experimental results of metallic structure fabrications have been reported, there are still no reports realizing the feature size down to around 100 nm for 3D metallic structures fabricated by multiphoton photoreduction. The major problem that inhibited the nanoscale size was the unwanted growth of the metal nanoparticles during laser irradiation. Therefore, the main issue to gain the nanometer scale depends on a way to avoid this unwanted metal particle growth and produce smaller nanoparticles to serve as building blocks.

In this report, we present a means to gain small feature sizes in the fabrication of metallic structures with the aid of a surfactant as a metal growth inhibitor. The minimum size of the silver structure fabricated by the proposed method was finer than the diffraction limit of light. For the first time, we demonstrate that the feature size was reduced to 180 nm for 3D structures by laser fabrication. A feature size as small as 120 nm was also realized for 2D silver patterns on the substrate. We also propose an illustration of the mechanism for nanometer scale patterning of metallic structures in the multiphoton-induced reduction technique, and experimentally show how the growth-inhibiting effect of a surfactant aids in the nanopattering of metallic nanostructures. This technique is a promising candidate for producing condensed microconductive devices of unique designs, such as microelectromechnical systems[23,24] and metamaterials operating in the visible light frequency region.[11]

Structures consisting of silver nanoparticles were produced in the metal-ion aqueous solutions placed on a cover slip by irradiation with a mode-locked femtosecond laser (Ti:sapphire

[*] Dr. T. Tanaka
Metamaterials Laboratory, RIKEN
(The Institute of Physical and Chemical Research)
2-1 Hirosawa, Wako, Saitama 351-0198 (Japan)
E-mail: t-tanaka@riken.jp
Dr. T. Tanaka
PRESTO, Japan Science and Technology Agency
4-1-8 Honcho Kawaguchi, Saitama, 332-0012 (Japan)
Prof. X.-M. Duan, Y.-Y. Cao
Laboratory of Organic NanoPhotonics and
Key Laboratory of Photochemical Conversion and Functional Materials,
Technical Institute of Physics and Chemistry,
Chinese Academy of Sciences
Beijing 100190 (P. R. China)
E-mail: xmduan@mail.ipc.ac.cn
Prof. X.-M. Duan, Y.-Y. Cao, Dr. N. Takeyasu, Prof. S. Kawata
Nanophotonics Laboratory, RIKEN
(The Institute of Physical and Chemical Research)
2-1 Hirosawa, Wako, Saitama 351-0198 (Japan)
Prof. X.-M. Duan, Prof. S. Kawata
CREST, Japan Science and Technology Agency
4-1-8 Honcho Kawaguchi, Saitama, 332-0012 (Japan)
Y.-Y. Cao
Graduate School of Chinese Academy of Sciences
Beijing 100080 (P. R. China)
Prof. S. Kawata
Department of Applied Physics, Graduate School of Engineering
Osaka University
2-1 Yamadaoka, Suita, Osaka 565-0871 (Japan)

[**] This work was financially supported by the PRESTO and CREST projects of the Japan Science and Technology Agency as well as the International Cooperation Program under Grant No. 2008DFA02050 of MOST of China.

DOI: 10.1002/smll.200801179

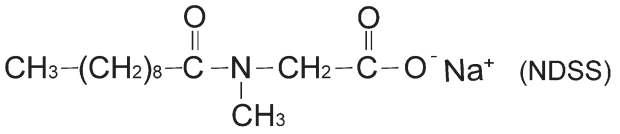

Scheme 1. Chemical structure of NDSS.

laser with an operating wavelength of 800 nm, a pulse width of 80 fs, and a repetition rate of 80 MHz). The laser light was introduced into an inverted microscope and tightly focused into the ion solution through the cover slip by an oil-immersion objective lens (60×, numerical aperture, $NA = 1.4$).[18] The laser power was controlled by a graduated neutral density filter. The focused laser light was scanned in 3D space by a computer-controlled motor-stage and galvanometer mirrors. Materials for photoreduction consisted of diammine silver ions (DSI) as the silver resource and a nitrogen-atom-containing alkyl carboxylate (n-decanoylsarcosine sodium, NDSS) as the surfactant, as illustrated in Scheme 1. This material was prepared by introducing varying amounts of NDSS into a prepared DSI solution. The concentration of silver ions in all the samples was 0.05 M.

Figure 1 shows the optical absorption spectra of pure NDSS, pure DSI, and the mixture of DSI and NDSS solutions. An absorption band whose peak is at 302 nm is seen in the spectra for both the pure DSI solution and the mixture of DSI and NDSS, but not in that for pure NDSS. This absorption band originates from the DSI itself. In all spectra, the remarkable absorption band is not observed at the laser wavelength of 800 nm. This implies that the photo-induced reduction reaction was associated with exciting the chemicals by the multiphoton absorption process.

To evaluate the function of NDSS molecules as an inhibitor for silver growth, samples with different NDSS concentrations of 0.013, 0.033, and 0.099 M were examined by drawing a line pattern under the same laser exposure conditions (scanning speed 6 μm s^{-1}, laser power 1.00 mW). Scanning electron microscope (SEM) images (as shown in Figure 2a–c) show that the widths of all strip patterns were around 300 nm at all concentrations of NDSS. The width of each metallic structure was clearly smaller than the size of the diffraction limit of 690 nm, which is given by $\approx 1.22\,\lambda\,NA^{-1}$. At the concentration of 0.013 M, the big particles with the diameter of more than one hundred nanometers were created on the fringe of the stripe, resulting from the low controllability on the particle growth by NDSS. However, when the concentration increased to 0.033 M, the size of the nanoparticles decreased to around 20 nm. When the concentration increased further to 0.099 M, the surface profile of the deposited silver became smooth and the size of the silver particles remained constantly 20 nm (as shown in Figure 2c). In this case, silver stripes consisted of densely packed nanoparticles with much sharper edges than those of the stripes obtained at the lower NDSS concentrations. These results imply that the formation of big particles was able to be prevented by the NDSS in the multiphoton absorption process, consistent with the findings in the synthesis of monodisperse silver nanocrystals using the stabilizer.[25]

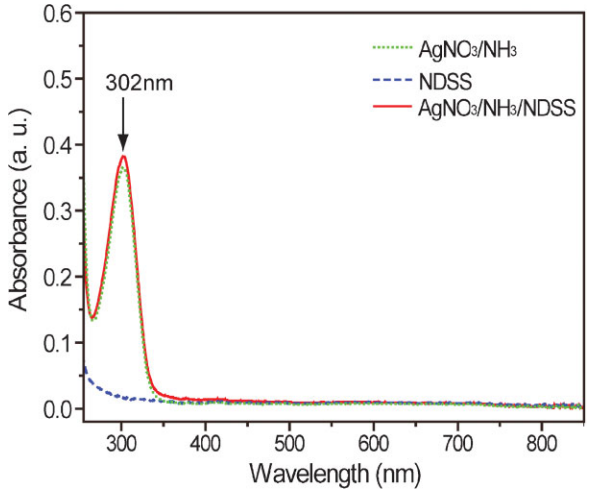

Figure 1. The optical absorption spectrum of the DSI aqueous solution with $[Ag^+] = 0.05$ M (dotted line), NDSS aqueous solution with [NDSS] = 0.4 M (dashed line), and the mixture of DSI and NDSS solution with [NDSS] = 0.099 M and $[Ag^+] = 0.05$ M (solid line).

In previous research on nanofabrication methods using a surfactant, the creation of nanoparticles/nanostructures has deeply depended on the formation of micelles.[6] In our case, when the NDSS concentrations were 0.013 and 0.033 M, which are lower than the critical micelle concentration (0.038 M),[26] silver stripes with a linewidth of 300 nm were fabricated. We concluded that the micelle formation of the surfactant is not the dominant factor of this resolution improvement. This result also agrees with the experimental phenomenon found in the synthesis of silver nanoparticles dispersed in aqueous solution using a laser.[27] Meanwhile, the degree of the particle aggregation became higher than that with low NDSS concentration, which led to a more continuous silver stripe. These results imply that the high NDSS concentration above the critical micelle concentration is better for improving the resolution and the continuity of the silver stripe.

In atomic force microscope (AFM) images (Figure 2d–f), the topography agrees well with the degree of the particle aggregation revealed by SEM images. Furthermore, cross-sectional images (Figure 2g–i) show that the height of the patterns increased from 60 nm to 194 nm with increasing concentrations of NDSS, indicating that the total amount of reduced silver increased. To confirm the existence of silver, energy dispersive X-ray spectroscopy (EDX) analysis was carried out on the patterns. The EDX results shown in Figure 2j reveal the existence of silver resulting from the photoreduction of silver ions.

To understand our experimental results, we divided the silver nanopattern formation into three stages as illustrated in Figure 3: nucleation of silver in stage 1, growth of nanoparticles in stage 2, and aggregation of silver nanoparticles in stage 3.

In the case of no NDSS, it has been found that a silver pattern with a lateral resolution of 1 μm consisted of large silver particles.[18] The nucleation process was initiated by laser irradiation, and afterwards the silver nuclei grew up to almost 1 μm. This ungoverned metal growth creates large-sized metal particles. After aggregation of the particles (stage 3), the existence of the large particles leads to thick

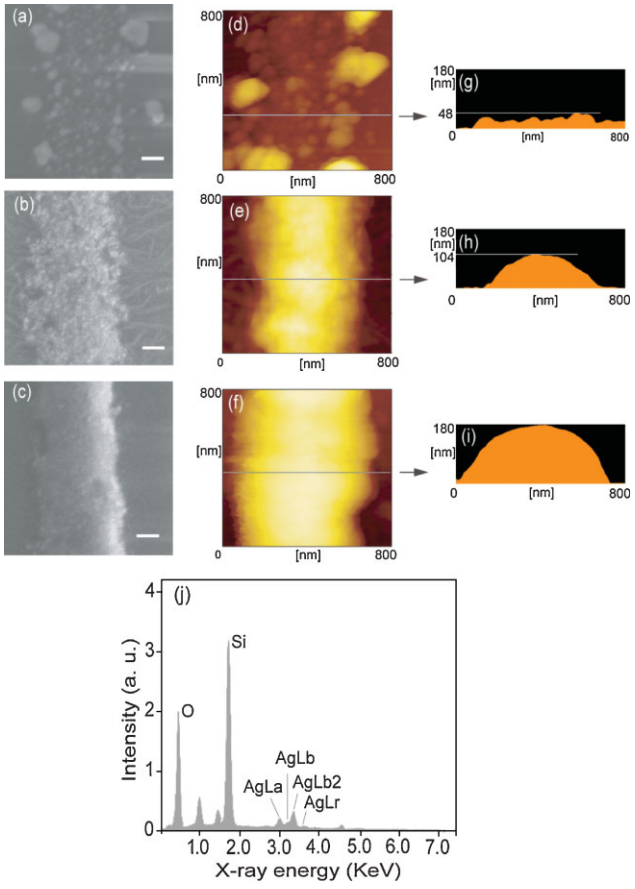

Figure 2. Relationship between the concentration of NDSS and the quality of silver patterns. The NDSS concentrations of 0.013, 0.033, and 0.099 M were selected for comparison under a certain concentration of Ag ions (0.05 M). The left part is SEM images obtained from samples with [NDSS] = 0.013 (a), 0.033 (b), and 0.099 (c) M, respectively; the right part shows corresponding topography (d–f) and cross-sectional images (g–i) taken by AFM. Scale bars are 100 nm in (a), (b), and (c). j) The EDX spectrum of the silver pattern, which confirmed the existence of silver nanoparticles.

silver lines and prevents the spatial resolution from reaching the hundred nanometer scale. On the other hand, when NDSS exists, even the probability of the nucleation is assumed to be the same, the NDSS molecules cover the surface of the silver particles immediately after the nucleation process and its cover layer eliminates further metal growth and decreases the particle size down to around 20 nm. In this case, the degree of particle growth suppression increases with increasing surfactant concentration. These growth-suppressed particles aggregate to compose silver patterns. In this stage, the concentration of particles is higher at the center of the focused laser spot, since there is a higher nucleation probability associated with the higher laser power. Meanwhile, the higher laser power also helps to break the surfactant layer[28] surrounding the particles, which in turn enhances the particle aggregation. These two conditions may lead to the aggregation of silver particles directed to the center of the laser beam.

We optimized experimental conditions, such as laser power, scanning velocity of the laser beam spot, and concentration of NDSS, to decrease the width of the lines. Since the growth of the nanoparticles was well-controlled and the degree of the particle aggregation was enhanced for the continuity of the silver stripe in the sample with the NDSS concentration of 0.099 M, this solution was used in the subsequent tests. As shown in Figure 4a, we drew silver lines on the glass substrate while varying the laser power from 0.87 mW to 1.35 mW and using a uniform scanning velocity of 6 $\mu m\ s^{-1}$. We found that the average width of the silver stripes was 500 nm when the applied laser power was 1.35 mW. The linewidth of the silver lines decreased with decreasing laser power, and at a laser power of 0.87 mW, a 120-nm line was obtained, as shown in Figure 4b and c.

To investigate the optical properties of the silver patterns, we fabricated a diffraction grating structure (as shown in Figure 5a). The pitch of adjacent lines was set to 5 μm, and the size of the structure was 1 mm × 1 mm (length × width). A HeNe laser was used for examining the transmission diffraction. From the diffraction images shown in Figure 5b, we observed clear and sharp diffracted laser beam spots up to 5th order. Furthermore, we introduced polarized light with an incident angle perpendicular to the silver grating and measured the polarized angle dependence of the transmission

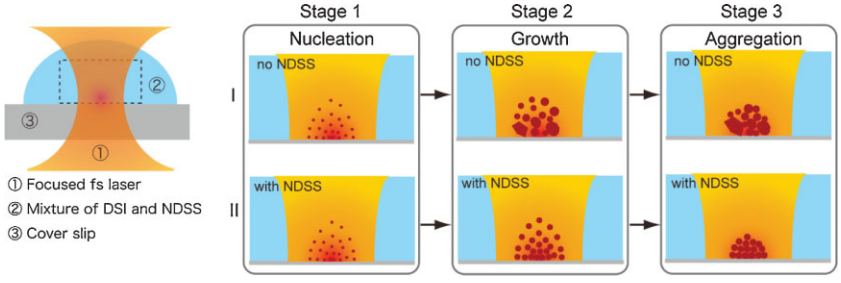

Figure 3. Schematic illustration of the formation of silver stripe patterns through the multiphoton-induced reduction process. The left scheme illustrates the photoreduction system. Routes I and II represent the patterning process of the samples with and without NDSS under the same laser power and exposure time. These two processes start from reduction of silver ions and the creation of silver seeds at stage 1 in the focal laser point. After that, the silver seeds grow up to nanoparticles at stage 2. In the absence of NDSS, varisized particles with different shapes are formed, whereas particles with uniform size and shape are created by adding NDSS. At stage 3, aggregation of the nanoparticles eventually leads to the formation of silver patterns.

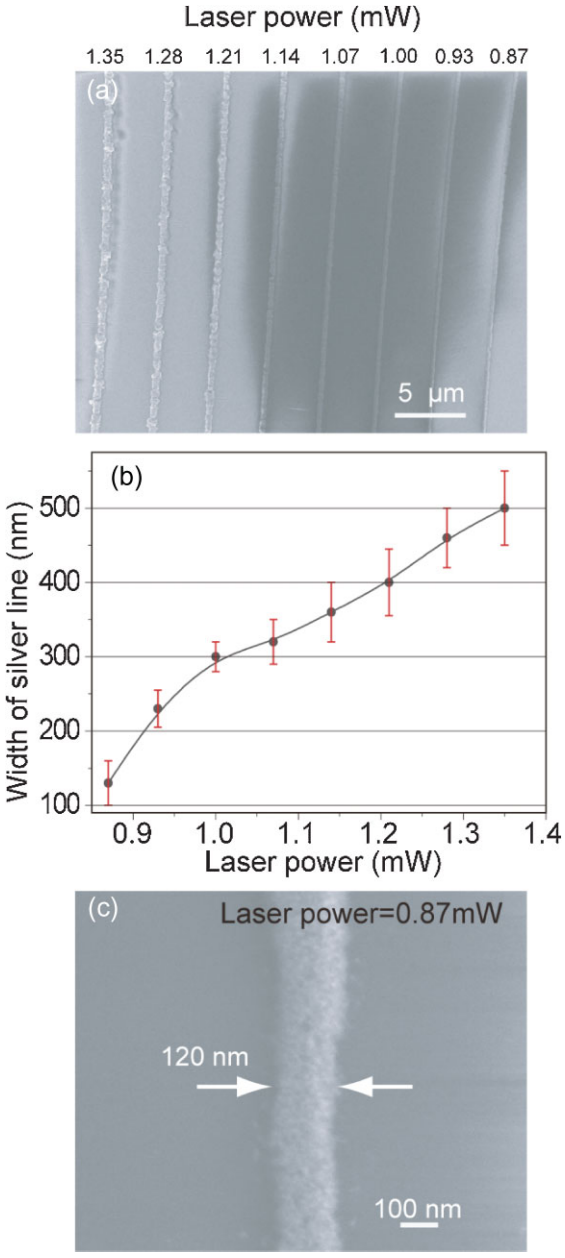

Figure 4. a) SEM image of silver stripe patterns formed using different laser powers and a linear scanning speed of 6 μm s^{-1}. b) Relationship between the laser power and width of the silver line from (a). c) Magnified image of a silver line (width 120 nm) fabricated using a laser power of 0.87 mW and a linear scanning speed of 6 μm s^{-1}.

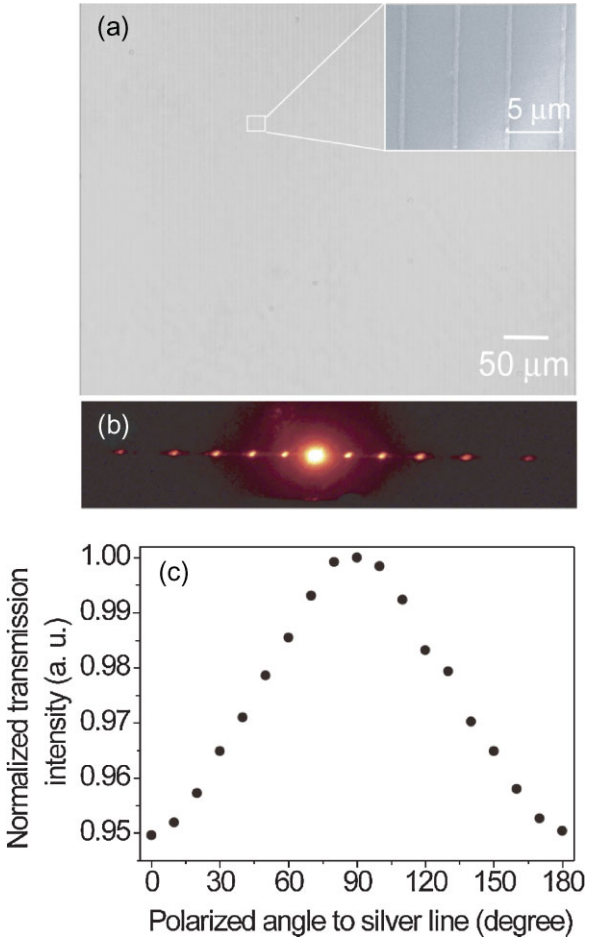

Figure 5. a) A reflection micrograph of a 1D silver grating with dimensions 1 mm × 1 mm (length × width) formed using a laser power of 1 mW and a linear scanning speed of 6 μm s^{-1}; the inset is a magnified SEM image showing the 5-μm period of the grating. b) The corresponding diffraction pattern observed in transmission. c) The normalized transmission intensity of light depending on the polarized angle in relation to the orientation of silver lines.

intensity of light. Here, we find in Figure 5c the total light intensity was the highest at the polarized angel of 90° and decreased by 5% at the polarized angles of 0° and 180°. This indicates that the silver grating acts as a light polarizer. These results imply the accuracy of the periodicity and continuity of the fabricated lines.

Figure 6a shows a free-standing silver pillar on the cover slip, which was obtained by scanning the focused laser spot along the direction normal to the plane of the cover slip. The silver pillar was created with a laser power of 1.14 mW and scanning speed of 3 μm s^{-1}. SEM images reveal that this pillar was measured with a minimum linewidth of 180 nm. Scanning the focused spot under the control of a computer enabled creation of 3D structures of arbitrary geometry. Figure 6b demonstrates the truly free-standing 3D silver pyramids fabricated with a scanning speed of 2.5 μm s^{-1} and laser power of 1.3 mW. These silver pyramids structures were strong enough to resist the surface tension in the washing process, which demonstrates that the silver particles were closely combined. The detail of the silver pyramid shown in Figure 6b reveals that the height was 5 μm and the angle for each edge relative to the substrate was 60°. Consequently, the direct photoreduction of the metal ions with surfactants could also lead to 3D metal structures with resolution exceeding the diffraction limit of light.

In conclusion, we have succeeded in fabricating silver structures with the minimum feature size smaller than 200 nm by a multiphoton-induced reduction technique combined with the inhibition of unwanted metallic particle growth through the use of surfactant. The surfactant molecules exhibited a significant contribution to the control of the diameters of nanoparticles down to tens of nanometers and they led to

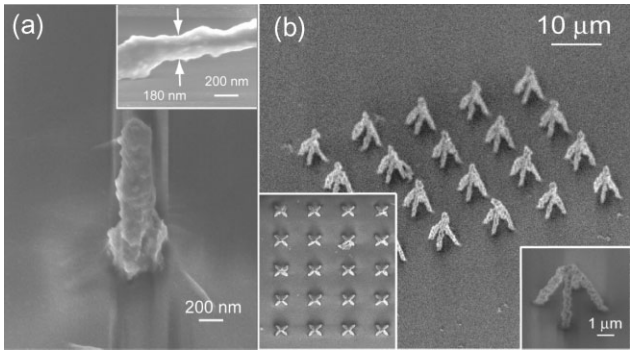

Figure 6. a) SEM image of the free-standing silver pillar on the cover slip, made by using a laser power of 1.14 mW and a linear scanning speed of 3 μm s^{-1}, taken at an observation angle of 45 °. The inset is a close-up view of the silver pillar parallel to the substrate, which demonstrates the linewidth of the smallest portion of the silver pillar as 180 nm. b) SEM image of silver pyramids, fabricated with a laser power of 1.3 mW and scanning speed of 2.5 μm s^{-1}, taken at an observation angle of 45 °. The inset on the left is a top view of the silver-pyramid array. The inset on the right is a close-up view of the silver pyramid.

achieving the silver stripe with the linewidth of 120 nm for the first time. Furthermore we have successfully fabricated free-standing 3D silver microstructures with the smallest size of 180 nm. Our approach not only illustrates an effective process for localized generation and aggregation of metal nanoparticles, but also offers a simple way to accurately control the location of nanoparticles on the nanometer scale. This finding may open the way to create arbitrary 3D metal structures and investigate unique functions of 3D metal structures in the nanoscale world.

Keywords:

metal · multiphoton process · nanostructures · photoreduction · surfactants

[1] S. Kawata, H. B. Sun, T. Tanaka, K. Takada, *Nature* **2001**, *412*, 697.
[2] W. H. Zhou, S. M. Kuebler, K. L. Braun, T. Y. Yu, J. K. Cammack, C. K. Ober, J. W. Perry, S. R. Marder, *Science* **2002**, *296*, 1106.
[3] S. Passinger, M. S. M. Saifullah, C. Reinhardt, K. R. V. Subramanian, B. N. Chichkov, M. E. Welland, *Adv. Mater.* **2007**, *19*, 1218.
[4] K. Kaneko, H. B. Sun, X. M. Duan, S. Kawata, *Appl. Phys. Lett.* **2003**, *83*, 1426.
[5] E. Hao, G. C. Schatz, *J. Chem. Phys.* **2004**, *120*, 357.
[6] C. Burda, X. B. Chen, R. Narayanan, M. A. El-Sayed, *Chem. Rev.* **2005**, *105*, 1025.
[7] H. Ohnishi, Y. Kondo, K. Takayanagi, *Nature* **1998**, *395*, 780.
[8] M. L. Brongersma, J. W. Hartman, H. A. Atwater, *Phys. Rev. B* **2000**, *62*, 16356.
[9] H. Ditlbacher, A. Hohenau, D. Wagner, U. Kreibig, M. Rogers, F. Hofer, F. R. Aussenegg, J. R. Krenn, *Phys. Rev. Lett.* **2005**, *95*, 257403.
[10] L. L. Yin, V. K. Vlasko-Vlasov, J. Pearson, J. M. Hiller, J. Hua, U. Welp, D. E. Brown, C. W. Kimball, *Nano Lett.* **2005**, *5*, 1399.
[11] A. Ishikawa, T. Tanaka, S. Kawata, *Phys. Rev. Lett.* **2005**, *95*, 237401.
[12] Y. L. Wu, Y. N. Li, B. S. Ong, *J. Am. Chem. Soc.* **2006**, *128*, 4202.
[13] J. R. Lakowicz, *Plasmonics* **2006**, *1*, 5.
[14] N. Toshima, *Supramol. Sci.* **1998**, *5*, 395.
[15] S. Subramanian, J. M. Catchmark, *Small* **2007**, *3*, 1934.
[16] K. Awazu, M. Fujimaki, C. Rockstuhl, J. Tominaga, H. Murakami, Y. Ohki, N. Yoshida, T. Watanabe, *J. Am. Chem. Soc.* **2008**, *130*, 1676.
[17] T. Baldacchini, A. C. Pons, J. Pons, C. N. LaFratta, J. T. Fourkas, Y. Sun, M. J. Naughton, *Opt. Express* **2005**, *13*, 1275.
[18] T. Tanaka, A. Ishikawa, S. Kawata, *Appl. Phys. Lett.* **2006**, *88*, 081107.
[19] S. Maruo, T. Saeki, *Opt. Express* **2008**, *16*, 1174.
[20] P. W. Wu, W. Cheng, I. B. Martini, B. Dunn, B. J. Schwartz, E. Yablonovitch, *Adv. Mater.* **2000**, *12*, 1438.
[21] F. Stellacci, C. A. Bauer, T. Meyer-Friedrichsen, W. Wenseleers, V. Alain, S. M. Kuebler, S. J. K. Pond, Y. D. Zhang, S. R. Marder, J. W. Perry, *Adv. Mater.* **2002**, *14*, 194.
[22] A. Ishikawa, T. Tanaka, S. Kawata, *Appl. Phys. Lett.* **2006**, *89*, 113102.
[23] M. Esashi, T. Ono, *J. Phys. D* **2005**, *38*, R223.
[24] E. Luber, R. Mohammadi, C. Ophus, Z. Lee, N. Nelson-Fitzpatrick, K. Westra, S. Evoy, U. Dahmen, V. Radmilovic, D. Mitlin, *Nanotechnology* **2008**, *19*, 25705.
[25] T. Kempa, R. A. Farrer, M. Giersig, J. T. Fourkas, *Plasmonics* **2006**, *1*, 45.
[26] M. J. Rosen, *Surfactants and Interfacial Phenomenon*, 3rd ed., Wiley, New York 2004, p. 122.
[27] J. P. Abid, A. W. Wark, P. F. Brevet, H. H. Girault, *Chem. Commun.* **2002**, 792.
[28] K. Abe, T. Hanada, Y. Yoshida, N. Tanigaki, H. Takiguchi, H. Nagasawa, M. Nakamoto, T. Yamaguchi, K. Yase, *Thin Solid Films* **1998**, *327*, 524.

Received: August 12, 2008
Revised: November 14, 2008
Published online: March 16, 2009

